Palestinian Medical and Pharmaceutical Journal

Unveiling the Potential of Velvet Apple (*Diospyros discolor* Willd.) Fruit Extract and Gel Formulation: Phytochemical Screening, Antioxidant Evaluation, Network Pharmacology, and Molecular Docking

Bayu Febram Prasetyo[1]*, Daffa' Rizal Dzulfaqaar Alauddin[1], Ahmad Kurniawan[2], Rini Madyastuti Purwono[1]

Type: Full Article. Received: 14th Feb. 2026, Accepted: 27th Jul 2026.

Accepted Manuscript, In Press

Abstract: Velvet apple (*Diospyros discolor* Willd.) is a tropical fruit with potential bioactive constituents relevant to antioxidant-based topical applications. This study evaluated Velvet apple fruit extract and a 10% (w/w) gel formulation through qualitative phytochemical screening, DPPH radical-scavenging assay, network pharmacology, and molecular docking. Fresh fruit pulp was taxonomically authenticated prior to extraction. The moisture content of the fresh fruit pulp was 82.13%, and maceration with 96% ethanol yielded 29.11% extract on a moisture-corrected basis. Qualitative phytochemical screening indicated the presence of flavonoids, tannins, and saponins. In the DPPH assay, the crude extract showed strong radical-scavenging activity with an IC_{50} of 46.00 ppm, compared with vitamin C at 5.60 ppm, whereas the gel formulation showed a much weaker apparent response under the assay conditions (IC_{50} = 33,286.00 ppm). In silico profiling of 52 putative constituents showed broad chemical diversity, with molecular weights ranging from 106.12 to 576.85 Da and topological polar surface area values from 0.00 to 190.28 Å^2. Target intersection analysis identified 95 shared proteins between predicted compound targets and wound-healing-related proteins, and enrichment analysis highlighted migration- and signaling-related processes. Network topology prioritized CASP3, and molecular docking against caspase-3 (PDB ID: 1NME) ranked bauerenol, β-amyrin, and cylindrin among the most plausible binders within the applied protocol. Overall, Velvet apple fruit extract appears to be a promising source of antioxidant phytochemicals, while the computational findings provide a predictive, hypothesis-generating basis for further wound-related investigation. Additional release studies, biological assays, and wound-healing models are needed to confirm formulation performance and biological relevance.

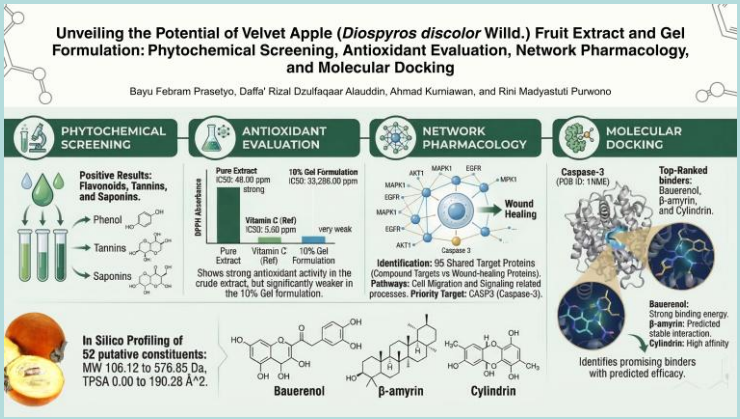

Keywords: wound healing, oxidative stress, tissue regeneration, topical therapeutics, caspase-3

Introduction

Plant-derived bioactive compounds have attracted considerable attention in wound-related research because they may provide multiple complementary effects, including antioxidant, anti-inflammatory, and antimicrobial activities, which are relevant to the complex nature of tissue repair [1,2]. Velvet apple (*Diospyros discolor* Willd.) is an underutilized tropical fruit with reported phytochemical richness and antioxidant potential. Previous studies on Velvet apple and related fruit extracts have indicated the presence of bioactive constituents and measurable radical-scavenging activity, supporting the plausibility of this species as a source of wound-relevant natural compounds [3,4].

Skin wounds remain a major clinical and public health challenge, particularly when healing is delayed or dysregulated. Chronic and difficult-to-heal wounds are associated with prolonged treatment, increased risk of infection, reduced quality of life, and substantial healthcare burden [5]. Successful wound healing depends on the coordinated progression of inflammation, cell migration, re-epithelialization, angiogenesis, and extracellular matrix remodeling; disruption of these events can impair closure and tissue restoration [6–8].

Oxidative stress remains a significant biological impediment to wound healing. Although physiological levels of reactive oxygen species (ROS) are essential for antimicrobial defense

[1] Division of Veterinary Pharmacy, School of Veterinary Medicine and Biomedical Sciences, IPB University, Bogor, Indonesia.
[2] Bachelor of Veterinary Medicine Study Program, School of Veterinary Medicine and Biomedical Sciences, IPB University, Bogor, Indonesia.
*Corresponding author: bayupr@apps.ipb.ac.id, ORCID: https://orcid.org/0000-0002-9026-5189

Published: An-Najah National University, Nablus, Palestine

and redox signaling, ROS overproduction prolongs inflammation and degrades critical cellular and extracellular matrix (ECM) components [9,10]. Consequently, antioxidant-based therapeutics have emerged as crucial strategies to ameliorate the wound microenvironment and restore redox homeostasis during tissue repair [11]. In this context, the antioxidant properties of Velvet apple present a promising therapeutic avenue. However, translating extract-level efficacy into topical utility necessitates an appropriate delivery system. Ideal wound-care vehicles must maintain prolonged local contact, preserve a moist microenvironment, and facilitate the targeted release of bioactive compounds [12]. Gel formulations offer an optimal matrix for this purpose, providing ease of administration, extended dermal residence time, and efficient localized delivery of therapeutic agents [13].

Given the multicomponent and multitarget nature of botanical extracts, elucidating their mechanisms necessitates systems-level approaches. Network pharmacology provides a robust framework for mapping complex compound-target-pathway interactions in phytomedicine [14,15]. In wound-healing research, integrating network pharmacology with molecular docking facilitates the identification of putative targets and plausible ligand-protein affinities [16,17]. However, as these in silico methods are inherently predictive and hypothesis-generating, their findings require careful interpretation and subsequent empirical validation to confirm pharmacological efficacy and mechanisms [18,19].

Consequently, this study investigated Velvet apple fruit extract and its gel formulation through phytochemical profiling, in vitro antioxidant assays, network pharmacology, and molecular docking. This integrative approach aimed to characterize the extract's antioxidant capacity, elucidate putative wound-healing mechanisms, and evaluate its suitability as a topical delivery system, thereby providing a robust theoretical foundation for subsequent empirical validation.

Materials and Methods

Materials

Fresh ripe Velvet apple (*Diospyros discolor* Willd.) fruits were collected from Institut Pertanian Bogor, Indonesia. The plant material was taxonomically authenticated at Research Center for Biology BRIN. After cleaning, the edible fruit material was separated, cut into small pieces, and used for simplicia preparation and extraction. Analytical-grade ethanol (96%) was used as the extraction solvent. Purified water/distilled water was used throughout the experimental procedures. For antioxidant analysis, 2,2-diphenyl-1-picrylhydrazyl (DPPH) and ascorbic acid (vitamin C) were used as the radical reagent and positive control standard, respectively, while ethanol was used as the reaction solvent. Analytical-grade reagents used for qualitative phytochemical screening included Dragendorff's, Mayer's, and Wagner's reagents (alkaloids); magnesium powder, hydrochloric acid, and amyl alcohol (flavonoids); 10% ferric chloride (tannins); anhydrous acetic acid and concentrated sulfuric acid (steroids/triterpenoids); and 10% sodium hydroxide (hydroquinones). Additional extraction solvents included ammonia, chloroform, ethanol, methanol, and diethyl ether. A Velvet apple topical gel was formulated by uniformly dispersing 4 g of the ethanol extract into 36 g of a pharmaceutical-grade base. The gel base comprised Carbopol 940 (gelling agent), propylene glycol (humectant), methylparaben (preservative), triethanolamine (pH adjuster), and purified water.

For the in silico study, putative phytochemical compounds of *Diospyros discolor* were compiled from TCMSP v3.0, ETCM v2.0, IMPPAT v2.0, and the KNApSAcK Family database. Chemical structures and identifiers were cross-checked using PubChem. Target prediction and annotation were conducted using SwissTargetPrediction, UniProt, GeneCards version 5.26.0, and DrugBank version 5.1.14. Network analyses were performed in Cytoscape version 3.10.3 using the CytoNCA and cytoHubba plugins. Functional enrichment was carried out using ShinyGO v0.85.1 with Homo sapiens selected as the organism. Molecular docking was performed in YASARA Structure v19.9.17, and molecular interaction figures were prepared using BIOVIA Discovery Studio Visualizer 2016 and PyMOL v3.1.5.1. All databases and software were accessed in February 2026.

Methods

Plant material and authentication

Fresh ripe Velvet apple (*Diospyros discolor* Willd.) fruits were obtained from Institut Pertanian Bogor, Indonesia. The plant material was authenticated at the Research Center for Biology BRIN, Cibinong, Indonesia, and the confirmed taxon was recorded as *Diospyros discolor* Willd. The fruits were washed with running water, drained, and the edible portion was separated for further processing. The plant identity was used consistently throughout the study to avoid confusion with the synonym *Diospyros blancoi*.

Preparation of simplicia and extraction

Fresh ripe Velvet apple (*Diospyros discolor* Willd.) fruits were washed with running water and drained thoroughly. The pulp was separated from the peel and seeds, cut into small pieces, and blended to obtain a homogeneous fruit mass. Five hundred grams of the blended pulp were subjected to maceration with 96% ethanol at a ratio of 1:10 (w/v). Extraction was carried out for 72 h at room temperature, with solvent renewal and filtration every 24 h. The combined filtrates were concentrated under reduced pressure until a viscous extract was obtained, and the final extract was weighed.

Determination of moisture content

The moisture content of Velvet apple fruit was determined by the gravimetric oven-drying method. Fresh fruits were washed with running water, drained, and the pulp was separated from the peel and seeds. The pulp was used as the sample for analysis. A porcelain dish was dried at 105 °C for 30 min, cooled in a desiccator for 30 min, and weighed. Approximately 2 g of fresh fruit pulp was then transferred into the dish and dried in an oven at 105 °C to constant weight. After each drying step, the dish was cooled in a desiccator for 30 min before reweighing.

Gel formulation

The topical gel was formulated at a 10% (w/w) concentration by incorporating Velvet apple ethanol extract into a pharmaceutical-grade gel base at a 1:9 ratio. Briefly, 4 g of Velvet apple ethanol extract was mixed with 36 g of gel base containing Carbopol 940 as the gelling agent, propylene glycol as the humectant, methylparaben as the preservative, triethanolamine (TEA) as the pH-adjusting agent, and purified water as the vehicle. Carbopol 940 was first dispersed in purified water and allowed to hydrate for 30 min. Methylparaben was dissolved in propylene glycol, after which the Velvet apple extract was incorporated into this phase. The hydrated Carbopol

dispersion was then combined gradually with the extract-containing phase under continuous stirring. Triethanolamine was added dropwise until the gel structure formed and the desired pH was achieved. Stirring was continued until a macroscopically homogeneous gel was obtained.

Qualitative phytochemical screening

The Velvet apple ethanol extract was subjected to qualitative phytochemical screening for alkaloids, flavonoids, tannins, saponins, triterpenoids, steroids, and hydroquinones using standard color and precipitation tests. For alkaloid screening, 1 g of sample was treated with ammonia, extracted with chloroform, acidified with 2 M sulfuric acid, and tested separately with Dragendorff's, Mayer's, and Wagner's reagents. Positive reactions were indicated by orange coloration, white precipitate, and brown coloration, respectively.

For flavonoid, tannin, and saponin screening, 5 g of sample was mixed with distilled water, heated for 5 min, and filtered. The filtrate was divided into three portions. Flavonoids were identified using magnesium powder, HCl:EtOH (1:1), and amyl alcohol, with orange coloration indicating a positive result. Tannins were identified by the addition of 10% $FeCl_3$, which produced a greenish-black coloration. Saponins were identified by the formation of stable foam after shaking.

For triterpenoid and steroid screening, 1 g of sample was extracted with hot ethanol, filtered, evaporated to dryness, redissolved in diethyl ether, and reacted with concentrated sulfuric acid and acetic anhydride. Red/purple coloration indicated triterpenoids, whereas green/blue coloration indicated steroids. Hydroquinones were screened by heating 1 g of sample in methanol, filtering, and adding 10% NaOH; a red coloration indicated a positive result. Results were recorded qualitatively as present (+) or absent (−).

DPPH radical-scavenging assay

The antioxidant capacity of the Velvet apple extract and its gel formulation was evaluated using a 96-well microplate DPPH assay. Briefly, the extract and ascorbic acid (positive control) were dissolved in DMSO and serially diluted to final test concentrations of 50–250 ppm and 1.25–20 ppm, respectively. For the formulated gel, the sample was prepared by homogeneously dispersing 1 g of the gel in 10 mL of ethanol under sonication, followed by dilution to the required test concentrations.

In each microplate well, 100 µL of the sample or control solution was mixed with 100 µL of a 125 µM DPPH ethanolic solution. Negative controls (ethanol and DPPH) and sample blanks (sample and ethanol) were prepared concurrently to correct for inherent sample absorbance. Following a 30-minute incubation in the dark at room temperature, the absorbance was measured at 517 nm using a microplate reader. The scavenging activity was subsequently calculated, and the IC_{50} values were determined. The percentage of DPPH radical inhibition was calculated using the following equation:

$$\%\ inhibition = \frac{A_{control} - A_{corrected\ sample}}{A_{control}} \times 100$$

Collection and Curation of *Diospyros discolor* Compounds

Putative phytochemicals of *Diospyros discolor* (syn. *Diospyros blancoi*) were retrieved from the TCMSP (v3.0), ETCM (v2.0), IMPPAT (v2.0), and KNApSAcK databases. Compounds lacking defined chemical structures or verified taxonomic origins were excluded. Overlapping entries across databases were deduplicated by matching canonical SMILES and InChIKeys. To resolve inter-database conflicts and standardize the dataset, all chemical identifiers (PubChem CID, canonical SMILES, and 3D conformers) were cross-validated using PubChem. The PubChem-verified structures were strictly retained as reference entries, yielding a curated, non-redundant compound library for subsequent in silico analyses.

In silico Physicochemical Profiling

The physicochemical properties of the curated compounds were evaluated using the SwissADME web tool. Key computed parameters included molecular weight (MW, Da), hydrogen bond acceptors (HBA) and donors (HBD), topological polar surface area (TPSA, Å²), rotatable bonds, PAINS alerts, and Lipinski's Rule of Five violations. To preserve the natural chemical diversity of the botanical extract, compounds were not strictly excluded based on isolated rule violations; rather, these descriptors were utilized exclusively for qualitative prioritization and compound profiling.

Prediction of compound targets and retrieval of wound-healing-related targets

Putative human protein targets for the curated compounds were identified using SwissTargetPrediction (*Homo sapiens*). To balance prediction sensitivity and specificity, a probability threshold of ≥ 0.10 was applied, retaining a maximum of 100 top-ranked targets per compound. This cutoff is established in network pharmacology to filter out low-confidence interactions while preserving structurally relevant targets [20]. All retrieved targets were standardized to official gene symbols using the UniProtKB database.

Disease-associated genes were retrieved from the GeneCards database using the keyword "wound healing". A relevance score cutoff of ≥ 3 was applied to isolate highly correlated therapeutic targets and eliminate peripheral gene associations [21,22]. The intersection between the compound-derived targets and the wound-healing genes was mapped using Venny v2.1.0, yielding the core target set for subsequent network construction and enrichment analyses.

Protein-Protein Interaction (PPI) Network and Enrichment Analysis

The intersected genes were mapped in the STRING v12.0 database (*Homo sapiens*) to construct a protein-protein interaction (PPI) network. The network topology was visualized and analyzed using Cytoscape v3.10.3. Hub proteins were identified via the cytoHubba plugin, utilizing *Degree* as the primary ranking metric, supported by *Betweenness* and *Closeness* centralities to ensure ranking robustness. Functional enrichment analysis, encompassing Gene Ontology (GO) terms and KEGG pathways, was executed using ShinyGO v0.85.1. Statistical significance was defined by a false discovery rate (FDR) ≤ 0.05. To minimize bias and ensure biological relevance, the analysis was strictly limited to gene set sizes of 10–500 and a fold enrichment ≥ 1.5 [23].

Molecular Docking and Protocol Validation

Molecular docking against caspase-3 (CASP3 with PDB ID: 1NME) was performed using YASARA Structure v19.9.17. Receptor preparation involved isolating the relevant monomeric

chain, depleting crystallographic waters and non-essential heteroatoms, adding polar hydrogens, and assigning physiological protonation states.

Docking simulations utilized the AutoDock Vina algorithm integrated within YASARA. The search space was strictly centered on the centroid of the co-crystallized native ligand (X: 29.70, Y: 29.70, Z: 29.70) with an 11 Å padding in all directions to fully encompass the active site. The protocol was prospectively validated by redocking the native ligand, which successfully reproduced the experimental binding mode with a root mean square deviation (RMSD) of 1.45 Å (threshold ≤ 2.0 Å).

For the test compounds, docking parameters were configured with an exhaustiveness of 8, a maximum of 10 modes, and a 3 kcal/mol energy range. Each ligand was subjected to three independent runs using distinct random seeds to minimize stochastic variation. The conformation exhibiting the lowest binding free energy (ΔG kcal/mol) and consistent active-site localization was selected. The 3D binding complexes and 2D ligand-residue interactions were visualized using PyMOL v3.1.5.1 and BIOVIA Discovery Studio Visualizer 2016.

Statistical Analysis

All in vitro experiments were performed in triplicate, and quantitative data are presented as the mean ± standard deviation (SD). The IC_{50} values for the DPPH assay were determined via linear regression analysis using Microsoft Excel.

Results and Discussion

Plant Material and Authentication

Botanical authentication confirmed the specimen as *Diospyros discolor* Willd. Explicitly establishing this identity is critical for taxonomic traceability, as the species is frequently cited in the literature under its accepted synonym, *Diospyros blancoi* [24]. Resolving this nomenclature ambiguity prevents inconsistencies in phytochemical profiling and ensures reliable pharmacological comparisons with prior studies.

Moisture Content and Extract Yield

The moisture content of the fresh Velvet apple fruit pulp was determined to be 82.13%. This value aligns perfectly with the naturally high aqueous composition (80–96%) characteristic of fresh postharvest fruits and vegetables [25]. Consequently, the obtained extract yield of 29.11% (w/w) strictly reflects the recovery efficiency from fresh botanical material, distinguishing it from yields typically derived from dried simplicia.

Table (1): Moisture Content of Crude Drugs and Yield of Velvet Apple Extract

Testing	Results (%)
Moisture content	82.13
Extract yield	29.11

Phytochemical Screening

Phytochemical profiling of the Velvet apple ethanol extract confirmed the presence of flavonoids, tannins, and saponins (Table 2). This specific metabolite signature is highly conducive to tissue repair; flavonoids are potent modulators of the wound healing cascade, actively promoting antioxidant, anti-inflammatory, angiogenic, and re-epithelialization pathways [2]. Concurrently, tannins synergize these effects through their robust antioxidant and antimicrobial capacities, while saponins further protect the wound microenvironment via membrane-disruptive antimicrobial mechanisms [26,27]. Although these preliminary colorimetric assays provide foundational evidence for the presence of these bioactive classes, subsequent quantitative and chromatographic analyses are required to elucidate precise compound identities and abundances.

Table (2): Phytochemical content of Velvet Apple Extract

Parameters	Results
Flavonoids	+
Alkaloids	-
Tannins	+
Saponins	+
Quinones	-
Steroids	-
Triterpenoids	-

Antioxidant activity of the extract and gel formulation

The DPPH radical-scavenging assay demonstrated a concentration-dependent inhibitory effect, with IC_{50} values of 5.60 ppm, 46.00 ppm, and 33,286.00 ppm for ascorbic acid (positive control), the Velvet apple extract, and the gel formulation, respectively (Figure 1). The robust antioxidant capacity of the crude extract (IC_{50} = 46.00 ppm) aligns closely with previous reports for *Diospyros discolor* ethanol extracts (IC_{50} ≈ 53.51 ppm), confirming the abundance of potent redox-active constituents [3].

Conversely, the remarkably high IC_{50} value of the gel formulation does not indicate a degradation of intrinsic antioxidant activity during preparation. Rather, this apparent reduction in efficacy may reflect limited analyte release from the polymer matrix and/or matrix interference under the assay conditions. The physical entrapment of the extract within the viscous polymeric matrix significantly limits its diffusion and accessibility to the DPPH radicals in the reaction medium. Furthermore, the DPPH assay is inherently highly sensitive to matrix interference, solvent polarity, and sample phase variations [28,29]. Therefore, the observed gel response reflects assay-accessibility limitations rather than an absolute loss of pharmacological potential, underscoring the necessity of prior in vitro release/extraction protocols when evaluating polymeric matrices.

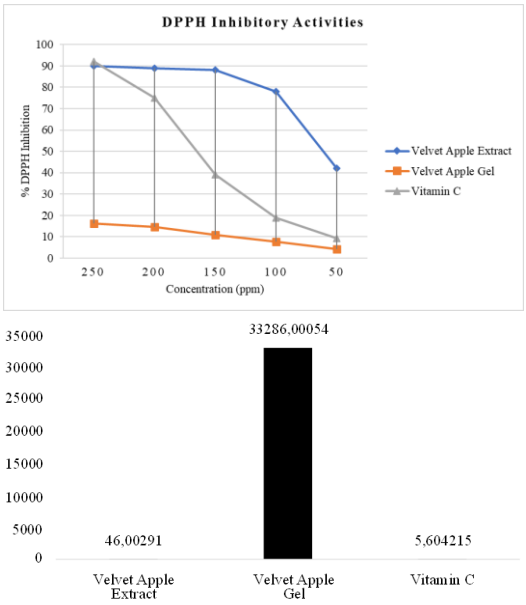

Figure (1): DPPH inhibitory activities and IC_{50} Values of Velvet apple extract, Velvet apple gel, and Vitamin C

Physicochemical Profiling of Putative Constituents

In silico physicochemical profiling utilizing the SwissADME platform demonstrated that the putative Velvet apple constituents span an extensive and diverse chemical space [30]. The compound library exhibited significant variations in molecular weight, topological polar surface area, hydrogen-bonding capacity, and molecular flexibility (rotatable bonds) (Table 3). While these descriptors are conventionally applied to predict systemic bioavailability via Lipinski's and Veber's rules, or to flag non-specific interactions using PAINS filters, their primary utility in the present study is to rigorously characterize the extract's structural heterogeneity [31–33].

Table (3): ADMET profile and druglikeness of compounds in *Diospyros discolor* Willd

No.	Ligands	Molecular Weight (Da)	Hydrogen Bond Acceptor	Hydrogen Bond Donor	Rotatable bond	Topological Polar Surface Area (Å²)	Lipinski #violations	PAINS #alerts
1.	(-)-β-Sitosterol	414.71	1	1	6	20.23	1	0
2.	(E)-Nerolidol	222.37	1	1	7	20.23	0	0
3.	1-Hexacosanol	382.71	1	1	24	20.23	1	0
4.	1,3,5,8-Tetrahydroxy-6-methoxy-2-methylanthraquinone	316.26	7	4	1	124.29	0	1
5.	6-(1,8-Dihydroxy-6-methylnaphthalen-2-yl)-5-hydroxy-2-methylnaphthalene-1,4-dione	360.36	5	3	1	94.83	0	2
6.	α-Amyrenone	424.7	1	0	0	17.07	1	0
7.	α-Amyrin	426.72	1	1	0	20.23	1	0
8.	α-Cadinol	222.37	1	1	1	20.23	0	0
9.	α-Humulene	204.35	0	0	0	0	1	0
10.	Anthraquinone	208.21	2	0	0	34.14	0	1
11.	Astragalin	448.38	11	7	4	190.28	2	0
12.	Bauerenol	426.72	1	1	0	20.23	1	0
13.	Benzaldehyde	106.12	1	0	1	17.07	0	0
14.	Benzyl benzoate	212.24	2	0	4	26.3	0	0
15.	Benzyl butyrate	178.23	2	0	5	26.3	0	0
16.	Benzyl salicylate	228.24	3	1	4	46.53	0	0
17.	β-Amyrin	426.72	1	1	0	20.23	1	0
18.	β-Betulinic acid	456.7	3	2	2	57.53	1	0
19.	β-caryophyllene	204.35	0	0	0	0	1	0
20.	β-sitosterol-3-O-glucopyranoside	576.85	6	4	9	99.38	1	0
21.	Betulin	442.72	2	2	2	40.46	1	0
22.	Betulinaldehyde	440.7	2	1	2	37.3	1	0
23.	Betulinic acid	456.7	3	2	2	57.53	1	0
24.	Betulinic acid methyl ester	547.79	6	1	3	90.08	2	0
25.	Butyl benzoate	178.23	2	0	5	26.3	0	0
26.	Butyl butyrate	144.21	2	0	6	26.3	0	0
27.	Cinnamyl benzoate	238.28	2	0	5	26.3	0	0
28.	Cinnamyl butyrate	204.26	2	0	6	26.3	0	0
29.	Cinnamyl valerate	218.29	2	0	7	26.3	0	0
30.	Cylindrin	440.74	1	0	2	9.23	1	0
31.	D-Galactose	180.16	6	5	1	110.38	0	0
32.	D-Galacturonic Acid	194.14	7	5	1	127.45	0	0
33.	D-Glucose	180.16	6	5	1	110.38	0	0
34.	D-Xylose	150.13	5	4	0	90.15	0	0
35.	Diospyrin	374.34	6	2	1	108.74	0	2
36.	Ellagic acid	302.19	8	4	0	141.34	0	1
37.	Ethyl palmitate	284.48	2	0	16	26.3	1	0
38.	Farnesol	222.37	1	1	7	20.23	1	0
39.	Hexadecanoic	388.54	5	1	18	71.25	1	0
40.	Hexadecanoic acid	256.42	2	1	14	37.3	1	0
41.	Hexyl benzoate	206.28	2	0	7	26.3	0	0
42.	L-(+)-Arabinose	150.13	5	4	4	97.99	0	0
43.	L-Rhamnose	164.16	5	4	0	90.15	0	0
44.	Lupeol	426.72	1	1	1	20.23	1	0
45.	Methyl benzoate	136.15	2	0	2	26.3	0	0
46.	Methyl palmitate	270.45	2	0	15	26.3	1	0
47.	Octyl benzoate	234.33	2	0	9	26.3	0	0
48.	Phenethyl butyrate	192.25	2	0	6	26.3	0	0
49.	Physostigmine	275.35	3	1	3	44.81	0	0

No.	Ligands	Molecular Weight (Da)	Hydrogen Bond Acceptor	Hydrogen Bond Donor	Rotatable bond	Topological Polar Surface Area (Å²)	Lipinski #violations	PAINS #alerts
50.	Stigmast-4-en-3-one	412.69	1	0	6	17.07	1	0
51.	Stigmasterol	412.69	1	1	5	20.23	1	0
52.	Ursolic acid	456.7	3	2	1	57.53	1	0

Intersected targets and enrichment analysis

Target intersection analysis revealed 95 overlapping proteins between the predicted targets of Velvet apple constituents and established wound-healing-associated genes. This multitarget profile perfectly aligns with the physiological complexity of wound repair, which requires the coordinated regulation of inflammation, angiogenesis, extracellular matrix (ECM) remodeling, and tissue maturation [34,35].

The identified network encompasses critical regulatory hubs across these distinct healing phases. Key intersections include matrix-remodeling enzymes (MMPs), receptor tyrosine kinases driving epithelialization and fibroblast transition (EGFR, PDGFRA, PDGFRB), and primary mediators of angiogenesis (KDR, FLT1, FGFR1) [36–39]. Additionally, the network highlights crucial inflammatory modulators (PTGS2, ICAM1) and central intracellular signaling nodes (AKT1, MAPKs, SRC, CASP3) [40–44]. Collectively, this broad target enrichment indicates that Velvet apple phytocompounds likely facilitate wound resolution by synergistically modulating multiple converging pathways rather than acting through a single dominant mechanism [16].

While these systems-level findings offer a robust biological rationale for the extract's therapeutic potential, they represent computational predictions. Consequently, this target network serves as a foundational, hypothesis-generating framework to prioritize specific pharmacological pathways for subsequent in vitro and in vivo validation [17].

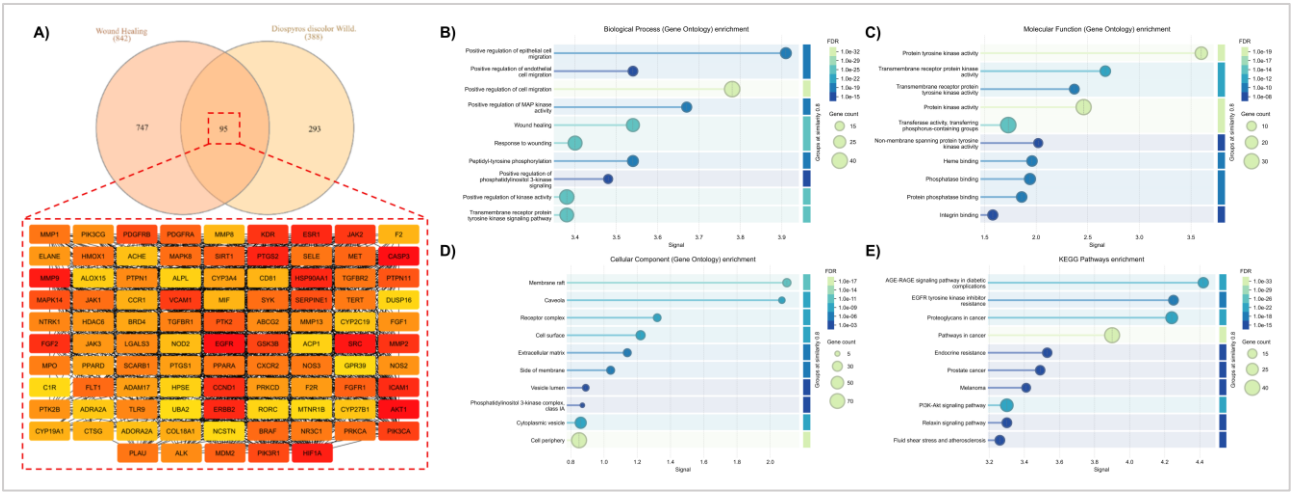

Figure (2): (A) Target protein from intersection analysis of *Diospyros discolor* Willd compounds and target protein of Wound Healing and Gene Ontology (GO) (B) categories Biological Process, (C) Molecular Function, (D) Cellular Component, and (E) Kyoto Encyclopedia of Genes and Genomes (KEGG) Pathway

GO and KEGG Enrichment Analysis

Functional enrichment analysis (GO and KEGG) revealed a significant clustering of targets within pathways fundamental to tissue repair (Figure 2). Highly enriched biological processes included epithelial and endothelial cell migration, response to wounding, and overall wound healing, which are critical drivers of tissue closure and re-epithelialization [6,7]. Furthermore, the overrepresentation of receptor-associated and kinase-linked signaling networks (PI3K/Akt) highlights a regulatory landscape that coordinates cellular proliferation, angiogenesis, and migration [42,43].

The pronounced enrichment of integrin-mediated signaling and extracellular matrix (ECM) organization strongly corroborates these findings. Integrins act as crucial mechanotransducers that facilitate keratinocyte motility, dynamic wound-bed interactions, and subsequent ECM remodeling during the proliferative phase of healing [8,45]. While these statistical associations robustly map the phytocompound targets to specific wound-relevant modules, they inherently serve as a predictive model for pathway prioritization. Subsequent empirical validation is essential to determine the precise pharmacological direction and magnitude of these modulatory effects.

Topological Screening and Key Target Prioritization

Topological analysis of the protein-protein interaction (PPI) network identified CASP3 as the paramount central node, exhibiting the highest degree, betweenness, and closeness centralities (Table 4). In complex biological networks, such highly connected nodes function as critical regulatory hubs or informational bottlenecks that orchestrate signaling crosstalk across diverse functional modules [46,47]. Consequently, CASP3 emerges as a pivotal convergence point within the predicted wound-healing network modulated by Velvet apple phytocompounds.

The prioritization of CASP3 perfectly aligns with the intricate, biphasic role of apoptosis during tissue repair. Apoptosis is not inherently detrimental; it is strictly required for the timely

resolution of inflammation (via immune cell clearance) and the orderly transition into the remodeling phase [44]. Conversely, excessive or dysregulated apoptosis can severely impair keratinocyte migration and delay re-epithelialization [48]. Crucially, targeted *in vivo* ablation of executioner caspases (caspase-3 and caspase-7) has been shown to paradoxically hinder skin wound repair and diminish compensatory cell proliferation in damaged tissues [49]. Therefore, in the context of Velvet apple phytotherapy, CASP3 acts as a dynamic regulatory node requiring balanced, homeostatic modulation, rather than ubiquitous pharmacological suppression to facilitate an optimal microenvironment for tissue regeneration.

Table (4): Nodes in the regulatory network of Wound Healing target proteins based on topological parameters of Degree, Eigenvector, LAC (Local Average Connectivity), Betweenness, Closeness, and Network. Values are reported using a period as the decimal separator.

Gene	Degree	Eigenvector	LAC	Betweenness	Closeness	Network
CASP3	69.0	0.19724055	29.42029	0.37041208	0.44339624	63.30364

Molecular Docking and Interaction Analysis

The docking protocol was prospectively validated by redocking the co-crystallized native ligand into human caspase-3 (PDB ID: 1NME), successfully reproducing the experimental binding pose with an RMSD of 1.45 Å. The native ligand, serving as the interaction benchmark, exhibited the most favorable binding free energy (-8.4530 kcal/mol; predicted Ki = 0.637 µM). This strong affinity was primarily driven by a critical hydrogen bond with Arg207 (2.68 Å) and supplementary polar contacts with Asn208, Ser249, and Trp214, establishing a robust polar-anchoring profile. Among the Velvet apple constituents, bauerenol (-7.9230 kcal/mol; 1.557 µM), β-amyrin (-7.6830 kcal/mol; 2.335 µM), and cylindrin (-7.6030 kcal/mol; 2.673 µM) emerged as the top-ranked candidates. Unlike the native ligand, these triterpenoid-like compounds occupied the active site primarily through extensive hydrophobic packing rather than directed polar anchoring. They consistently interacted with key residues, including Tyr204, Trp206, Arg207, Asn208, Ser209, Ser249, Phe250, and Ser251. While this interaction signature aligns with the hydrophobic subsite architecture previously reported for non-peptidic caspase-3 ligands, other constituents like ursolic acid and α-amyrin displayed considerably weaker affinities and suboptimal polar contacts [50].

Table (5): Gibbs free energy (ΔG), Inhibition Constant values, and Amino acid residues from molecular docking of *Diospyros discolor* Willd test ligands against Caspase-3 (PDB ID: 1NME)

Ligands	Gibbs free energy (ΔG) (kcal/mol)	Inhibition Constant (µM)	Residues involved in molecular docking	
			Hydrophobic Interactions	Hydrogen Bonds
2-Hydroxy-5-(2-Mercapto-Ethylsulfamoyl)-Benzoic Acid*	-8.4530	0.637	Ser205 Tyr204 Ser209 Phe250 Ser251 Trp206	Arg207 (2.68 Å) Trp214 (5.07 Å) Asn208 (4.27 Å) Ser249 (3.92 Å)
Bauerenol	-7.9230	1.557	Lys210 Ser249 Phe250 Ser251 Asp211 Phe247 Trp214 Glu248 Asn208 Trp206 Arg207 Ser209 Tyr204	-
β-Amyrin	-7.6830	2.335	Tyr204 Phe256 Phe250 Ser249 Glu248 Arg207 Trp214 Asn208 Trp206 Ser209 Phe252 Ser251 Asp253	-
Cylindrin	-7.6030	2.673	Asp211 Phe252 Ser251 Asp253 Trp206 Arg207 Phe250 Asn208 Ser249 Ser209 Trp214 Glu248 Phe247 Glu246	-
Ursolic acid	-7.4480	3.472	Ser209 Asp211 Phe247 Glu246 Trp214 Ser249 Asn208 Phe250 Trp206 Ser251 Arg207	Glu248 (4.05 Å)
α-Amyrin	-7.2490	4.858	Gln217 Trp214 Asn208 Ser249 Glu248 Glu246 Phe247 Phe250	Asp211 (4.89 Å)

*Native Ligand

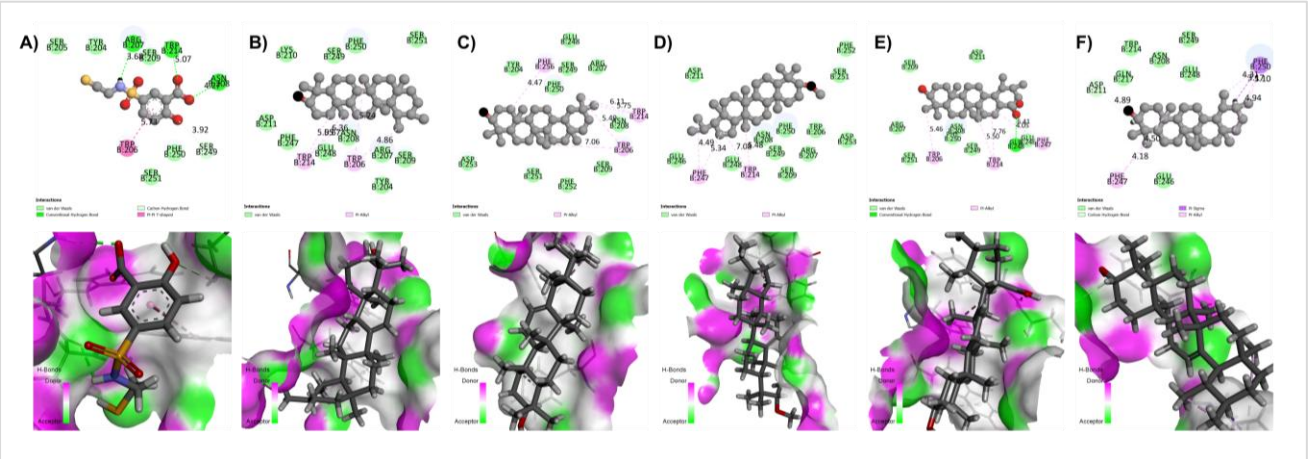

Figure (3): 2D and 3D interaction maps of the native ligand and selected Velvet apple compounds in the CASP3 binding pocket: (A) 2-hydroxy-5-(2-mercapto-ethylsulfamoyl)-benzoic acid (native ligand), (B) bauerenol, (C) β-amyrin, (D) cylindrin, (E) ursolic acid, and (F) α-amyrin. The native ligand showed stronger polar anchoring, whereas the phytochemical ligands were dominated mainly by hydrophobic contacts within the same general binding region.

Although the top phytocompounds exhibited favorable pocket occupancy, their binding scores remained naturally lower than the highly optimized native ligand. Contemporary benchmarking of docking scoring functions emphasizes their proficiency in pose generation and relative candidate prioritization, rather than absolute quantitative affinity prediction [51,52]. Furthermore, while the localized interactions suggest compatibility with the active site, definitive claims regarding dynamic conformational changes, such as induced-fit rearrangements of Tyr204 necessitate future molecular dynamics simulations. Therefore, within the broader wound-healing network, bauerenol, β-amyrin, and cylindrin are prioritized as highly plausible modulatory candidates that warrant subsequent in vitro enzymatic and cellular validation.

Conclusion

This study demonstrates that the ethanolic extract of fresh Velvet apple (*Diospyros discolor* Willd.) fruit is a rich source of redox-active phytochemicals specifically flavonoids, tannins, and saponins exhibiting potent in vitro antioxidant capacity. While the formulated topical gel displayed restricted radical-scavenging activity due to polymeric matrix entrapment, the intrinsic bioactivity of the botanical extract remains evident. Furthermore, integrated in silico network pharmacology and molecular docking analyses elucidated the extract's multitarget potential in tissue repair. We identified CASP3 as a pivotal regulatory hub and prioritized specific triterpenoids (bauerenol, β-amyrin, and cylindrin) as highly plausible modulators of critical wound-healing pathways, including angiogenesis, cell migration, and signaling regulation. Ultimately, these findings establish a robust structural and mechanistic framework for Velvet apple as a promising source of wound-relevant antioxidant phytochemicals and a candidate for further wound-related investigation. Future investigations should focus on optimizing the gel formulation to enhance active compound release, alongside rigorous *in vivo* and biochemical validation of the predicted pharmacological targets.

Disclosure Statements

Ethics approval and consent to participate

Ethical approval was not required because this study did not involve human participants, animal subjects, or any clinical data.

Consent for publication

Consent for publication was not required because this study did not include identifiable personal data, images, or case reports.

Availability of data and materials

The data supporting the findings of this study are provided within the manuscript text, tables, and figures. The protein structure used for molecular docking, caspase-3 (PDB ID: 1NME), is publicly accessible in the RCSB Protein Data Bank. Putative bioactive compounds were compiled from TCMSP v3.0, ETCM v2.0, IMPPAT v2.0, and the KNApSAcK Family database, while chemical structures and identifiers were obtained from publicly available resources including PubChem.

Author's contribution

Bayu Febram Prasetyo contributed to conceptualization, methodology, supervision, and manuscript review. Daffa' Rizal Dzulfaqaar Alauddin contributed to data curation, network pharmacology, molecular docking, visualization, and writing the original draft. Ahmad Kurniawan contributed to laboratory investigation, data collection, and formal analysis. Rini Madyastuti Purwono contributed to validation, supervision, and critical revision of the manuscript. All authors reviewed and approved the final manuscript.

Funding

The research did not receive any financial support.

Source of Research

This study was derived from an undergraduate research project conducted at the School of Veterinary Medicine and Biomedical Sciences, IPB University, Bogor, Indonesia.

Acknowledgments

The authors would like to thank the School of Veterinary Medicine and Biomedical Sciences, IPB University, for providing facilities and institutional support for this research.

Conflicts of interest

The authors declare that there is no conflict of interest regarding the publication of this article

References

[1] Carvalho MTB, Araújo-Filho HG, Barreto AS, Quintans-Júnior LJ, Quintans JSS, Barreto RSS. Wound healing properties of flavonoids: A systematic review highlighting the mechanisms of action. Phytomedicine 2021;90:153636. https://doi.org/10.1016/j.phymed.2021.153636.

[2] Zulkefli N, Che Zahari CNM, Sayuti NH, Kamarudin AA, Saad N, Hamezah HS, et al. Flavonoids as Potential Wound-Healing Molecules: Emphasis on Pathways Perspective. Int J Mol Sci 2023;24:4607. https://doi.org/10.3390/ijms24054607.

[3] Noviardi H, Ratu AP, Safitri AF. Isolasi Senyawa Antioksidan Ekstrak Etanol Buah Bisbul (*Diospyros discolor* Willd.). Jurnal Farmamedika 2018;3:82–9. https://doi.org/10.47219/ath.v3i2.15.

[4] Hossain MM, Rahim MA, Haque MR. Biochemical properties of some important underutilized minor fruits. J Agric Food Res 2021;5:100148. https://doi.org/10.1016/j.jafr.2021.100148.

[5] Sen CK. Human Wound and Its Burden: Updated 2022 Compendium of Estimates. Adv Wound Care (New Rochelle) 2023;12:657–70. https://doi.org/10.1089/wound.2023.0150.

[6] Pastar I, Stojadinovic O, Yin NC, Ramirez H, Nusbaum AG, Sawaya A, et al. Epithelialization in Wound Healing: A

Comprehensive Review. Adv Wound Care (New Rochelle) 2014;3:445–64. https://doi.org/10.1089/wound.2013.0473.
[7] Rousselle P, Braye F, Dayan G. Re-epithelialization of adult skin wounds: Cellular mechanisms and therapeutic strategies. Adv Drug Deliv Rev 2019;146:344–65. https://doi.org/10.1016/j.addr.2018.06.019.
[8] Diller RB, Tabor AJ. The Role of the Extracellular Matrix (ECM) in Wound Healing: A Review. Biomimetics 2022;7:87. https://doi.org/10.3390/biomimetics7030087.
[9] Ukaegbu K, Allen E, Svoboda KKH. Reactive Oxygen Species and Antioxidants in Wound Healing: Mechanisms and Therapeutic Potential. Int Wound J 2025;22:e70330. https://doi.org/10.1111/iwj.70330.
[10] Hunt M, Torres M, Bachar-Wikstrom E, Wikstrom JD. Cellular and molecular roles of reactive oxygen species in wound healing. Commun Biol 2024;7:1534. https://doi.org/10.1038/s42003-024-07219-w.
[11] Comino-Sanz IM, López-Franco MD, Castro B, Pancorbo-Hidalgo PL. The Role of Antioxidants on Wound Healing: A Review of the Current Evidence. J Clin Med 2021;10:3558. https://doi.org/10.3390/jcm10163558.
[12] Nuutila K, Eriksson E. Moist Wound Healing with Commonly Available Dressings. Adv Wound Care (New Rochelle) 2021;10:685–98. https://doi.org/10.1089/wound.2020.1232.
[13] Zhang H, Lin X, Cao X, Wang Y, Wang J, Zhao Y. Developing natural polymers for skin wound healing. Bioact Mater 2024;33:355–76. https://doi.org/10.1016/j.bioactmat.2023.11.012.
[14] Lee W-Y, Park K-I, Bak S-B, Lee S, Bae S-J, Kim M-J, et al. Evaluating current status of network pharmacology for herbal medicine focusing on identifying mechanisms and therapeutic effects. J Adv Res 2025;76:799–815. https://doi.org/10.1016/j.jare.2024.12.040.
[15] Noor F, Tahir ul Qamar M, Ashfaq UA, Albutti A, Alwashmi ASS, Aljasir MA. Network Pharmacology Approach for Medicinal Plants: Review and Assessment. Pharmaceuticals 2022;15:572. https://doi.org/10.3390/ph15050572.
[16] Ratha J, Padumanonda T, Yongram C, Siriparu P, Datham S, Subhan M, et al. Network Pharmacology of the Phytochemical Content of Sunflower Seed (Helianthus annuus L.) Extract from LC-MS on Wound-Healing Activity and the In Vitro Wound Scratch Assay. Plants 2026;15:187. https://doi.org/10.3390/plants15020187.
[17] Zhang Z, Wang L, Li X, Miao Y, Li D. Integrating Network Pharmacology, Molecular Docking and Experimental Validation to Explore the Pharmacological Mechanisms of Quercetin Against Diabetic Wound. Int J Med Sci 2024;21:2837–50. https://doi.org/10.7150/ijms.100468.
[18] Ramírez D, Caballero J. Is It Reliable to Use Common Molecular Docking Methods for Comparing the Binding Affinities of Enantiomer Pairs for Their Protein Target? Int J Mol Sci 2016;17:525. https://doi.org/10.3390/ijms17040525.
[19] Pantsar T, Poso A. Binding Affinity via Docking: Fact and Fiction. Molecules 2018;23:1899. https://doi.org/10.3390/molecules23081899.
[20] Guzmán-Flores JM, Pérez-Vázquez V, Martínez-Esquivias F, Isiordia-Espinoza MA, Viveros-Paredes JM. Molecular Docking Integrated with Network Pharmacology Explores the Therapeutic Mechanism of Cannabis sativa against Type 2 Diabetes. Curr Issues Mol Biol 2023;45:7228–41. https://doi.org/10.3390/cimb45090457.
[21] Zhang W, Ge H, Wei Y, Gao J, Tian F, Zhou E. Molecular characterization of PANoptosis-related genes in chronic kidney disease. PLoS One 2024;19:e0312696. https://doi.org/10.1371/journal.pone.0312696.
[22] Zhang D, Han L, Zhang W, Wang D, Huo D, Tan X, et al. Neuroprotective mechanisms of valproic acid and alpha-lipoic acid in ALS: a network pharmacology-based investigation. Front Pharmacol 2025;16:1681929. https://doi.org/10.3389/fphar.2025.1681929.
[23] Reimand J, Isserlin R, Voisin V, Kucera M, Tannus-Lopes C, Rostamianfar A, et al. Pathway enrichment analysis and visualization of omics data using g:Profiler, GSEA, Cytoscape and EnrichmentMap. Nat Protoc 2019;14:482–517. https://doi.org/10.1038/s41596-018-0103-9.
[24] Noviardi H, Ratnasari D, Fermadianto M. Formulasi Sediaan Krim Tabir Surya dari Ekstrak Etanol Buah Bisbul (Diospyros blancoi). Jurnal Ilmu Kefarmasian Indonesia 2019;17:262. https://doi.org/10.35814/jifi.v17i2.771.
[25] Zuo X, Wang J, Li Y, Zhang J, Wu Z, Jin P, et al. Recent advances in high relative humidity strategy for preservation of postharvest fruits and vegetables: A comprehensive review. Food Chem 2025;481:144130. https://doi.org/10.1016/j.foodchem.2025.144130.
[26] Cosme F, Aires A, Pinto T, Oliveira I, Vilela A, Gonçalves B. A Comprehensive Review of Bioactive Tannins in Foods and Beverages: Functional Properties, Health Benefits, and Sensory Qualities. Molecules 2025;30:800. https://doi.org/10.3390/molecules30040800.
[27] Li J, Monje-Galvan V. In Vitro and In Silico Studies of Antimicrobial Saponins: A Review. Processes 2023;11:2856. https://doi.org/10.3390/pr11102856.
[28] La J, Kim M-J, Lee J. Evaluation of solvent effects on the DPPH reactivity for determining the antioxidant activity in oil matrix. Food Sci Biotechnol 2021;30:367–75. https://doi.org/10.1007/s10068-020-00874-9.
[29] Gulcin İ, Alwasel SH. DPPH Radical Scavenging Assay. Processes 2023;11:2248. https://doi.org/10.3390/pr11082248.
[30] Daina A, Michielin O, Zoete V. SwissADME: a free web tool to evaluate pharmacokinetics, drug-likeness and medicinal chemistry friendliness of small molecules. Sci Rep 2017;7:42717. https://doi.org/10.1038/srep42717.
[31] Lipinski CA, Lombardo F, Dominy BW, Feeney PJ. Experimental and computational approaches to estimate solubility and permeability in drug discovery and development settings. Adv Drug Deliv Rev 2001;46:3–26. https://doi.org/10.1016/S0169-409X(00)00129-0.
[32] Veber DF, Johnson SR, Cheng H-Y, Smith BR, Ward KW, Kopple KD. Molecular Properties That Influence the Oral Bioavailability of Drug Candidates. J Med Chem 2002;45:2615–23. https://doi.org/10.1021/jm020017n.
[33] Baell JB, Holloway GA. New Substructure Filters for Removal of Pan Assay Interference Compounds (PAINS) from Screening Libraries and for Their Exclusion in Bioassays. J Med Chem 2010;53:2719–40. https://doi.org/10.1021/jm901137j.
[34] Jin C, Jin Y, Ding Z, Nuch KS, Han M, Shim J, et al. Cellular and Molecular Mechanisms of Wound Repair: From Biology to Therapeutic Innovation. Cells 2025;14:1850. https://doi.org/10.3390/cells14231850.
[35] Mamun A Al, Shao C, Geng P, Wang S, Xiao J. Recent advances in molecular mechanisms of skin wound healing and its treatments. Front Immunol 2024;15:1395479. https://doi.org/10.3389/fimmu.2024.1395479.
[36] Caley MP, Martins VLC, O'Toole EA. Metalloproteinases and Wound Healing. Adv Wound Care (New Rochelle) 2015;4:225–34. https://doi.org/10.1089/wound.2014.0581.
[37] Repertinger SK, Campagnaro E, Fuhrman J, El-Abaseri T, Yuspa SH, Hansen LA. EGFR Enhances Early Healing After Cutaneous Incisional Wounding. J Invest Dermatol 2004;123:982–9. https://doi.org/10.1111/j.0022-202X.2004.23478.x.
[38] Yao L, Rathnakar BH, Kwon HR, Sakashita H, Kim JH, Rackley A, et al. Temporal control of PDGFRα regulates the fibroblast-to-myofibroblast transition in wound healing.

Cell Rep 2022;40:111192. https://doi.org/10.1016/j.celrep.2022.111192.
[39] Chen J, Qin S, Xing Z, Peng C, Li D. Targeting angiogenesis in diabetic wound healing: New insight from chemical architecture to functional outcomes. J Pharm Anal 2026;16(6):101475. https://doi.org/10.1016/j.jpha.2025.101475.
[40] Bui TM, Wiesolek HL, Sumagin R. ICAM-1: A master regulator of cellular responses in inflammation, injury resolution, and tumorigenesis. J Leukoc Biol 2020;108:787–99. https://doi.org/10.1002/JLB.2MR0220-549R.
[41] Moon H, White AC, Borowsky AD. New insights into the functions of Cox-2 in skin and esophageal malignancies. Exp Mol Med 2020;52:538–47. https://doi.org/10.1038/s12276-020-0412-2.
[42] Teng Y, Fan Y, Ma J, Lu W, Liu N, Chen Y, et al. The PI3K/Akt Pathway: Emerging Roles in Skin Homeostasis and a Group of Non-Malignant Skin Disorders. Cells 2021;10:1219. https://doi.org/10.3390/cells10051219.
[43] Bonnici L, Suleiman S, Schembri-Wismayer P, Cassar A. Targeting Signalling Pathways in Chronic Wound Healing. Int J Mol Sci 2023;25:50. https://doi.org/10.3390/ijms25010050.
[44] Riwaldt S, Corydon TJ, Pantalone D, Sahana J, Wise P, Wehland M, et al. Role of Apoptosis in Wound Healing and Apoptosis Alterations in Microgravity. Front Bioeng Biotechnol 2021;9:679650. https://doi.org/10.3389/fbioe.2021.679650.
[45] Yu D, Lu Z, Nie F, Chong Y. Integrins regulation of wound healing processes: insights for chronic skin wound therapeutics. Front Cell Infect Microbiol 2024;14:1324441. https://doi.org/10.3389/fcimb.2024.1324441.
[46] Chen S-J, Liao D-L, Chen C-H, Wang T-Y, Chen K-C. Construction and Analysis of Protein-Protein Interaction Network of Heroin Use Disorder. Sci Rep 2019;9:4980. https://doi.org/10.1038/s41598-019-41552-z.
[47] Soofi A, Taghizadeh M, Tabatabaei SM, Tavirani MR, Shakib H, Namaki S, et al. Centrality Analysis of Protein-Protein Interaction Networks and Molecular Docking Prioritize Potential Drug-Targets in Type 1 Diabetes. Iran J Pharm Res 2020;19:121–34. https://doi.org/10.22037/IJPR.2020.113342.14242.
[48] Wu X, Gu R, Tang M, Mu X, He W, Nie X. Elucidating the dual roles of apoptosis and necroptosis in diabetic wound healing: implications for therapeutic intervention. Burns Trauma 2025;13:tkae061. https://doi.org/10.1093/burnst/tkae061.
[49] Walker D. Phoenix rising. Nat Rev Mol Cell Biol 2010;11:233. https://doi.org/10.1038/nrm2877.
[50] Ganesan R, Jelakovic S, Mittl PRE, Caflisch A, Grütter MG. In silico identification and crystal structure validation of caspase-3 inhibitors without a P1 aspartic acid moiety. Acta Crystallogr Sect F Struct Biol Cryst Commun 2011;67:842–50. https://doi.org/10.1107/S1744309111018604.
[51] Vittorio S, Lunghini F, Morerio P, Gadioli D, Orlandini S, Silva P, et al. Addressing docking pose selection with structure-based deep learning: Recent advances, challenges and opportunities. Comput Struct Biotechnol J 2024;23:2141–51. https://doi.org/10.1016/j.csbj.2024.05.024.
[52] Angelova M, Alov P, Tsakovska I, Jereva D, Lessigiarska I, Atanassov K, et al. Pairwise Performance Comparison of Docking Scoring Functions: Computational Approach Using InterCriteria Analysis. Molecules 2025;30:2777. https://doi.org/10.3390/molecules30132777.